Surface Science 603 (2009) 597–605

Contents lists available at ScienceDirect

Surface Science

journal homepage: www.elsevier.com/locate/susc

Neutralization of Li^+ ions scattered by the Cu (100) and (111) surfaces: A localized picture of the atom-surface interaction

Evelina A. García [a,*], M.A. Romero [a], C. González [b], E.C. Goldberg [a,c]

[a] Instituto de Desarrollo Tecnológico para la Industria Química (INTEC), Consejo Nacional de Investigaciones Científicas y Técnicas (CONICET), Güemes 3450 CC 91, 3000 Santa Fe, Argentina
[b] Czech Academy of Sciences, Institute of Physics, Department of Thin Films, Cukrovarnicka 10, 16253 Prague, Czech Republic
[c] Departamento Ing. Materiales, Facultad de Ing. Química, Universidad Nacional del Litoral, Santiago del Estero 2829, 3000 Santa Fe, Argentina

ARTICLE INFO

Article history:
Received 6 October 2008
Accepted for publication 16 December 2008
Available online 25 December 2008

Keywords:
Charge transfer
Alkali metals
Electron transfer
Neutralization mechanisms
Atom-solid interaction

ABSTRACT

Large and face dependent neutral fractions have been found recently in the scattering of Li^+ by Cu(100) and Cu(111) surfaces. These results for high work function surfaces are unexpected within the 'traditional' picture of a Li^+ ion departing from a jellium surface model. In the present work the Li^+/Cu(100) and Li^+/Cu(111) interacting systems are described by a previously developed *bond-pair* model based on the localized interactions between the projectile ion and the atoms of the surface, and on the extended features of the electronic band structure through the surface local density of states. By only including the resonant neutralization to the Li atom ground state we explained the face and energy dependences of the measured neutral fractions for large outgoing energy values. We found that the downward shift of the Li ionization level below the Fermi level caused by the short range chemical interactions, is the main responsible of a high neutralization by the resonant mechanism. The remaining differences between theory and experiment values can be explained in terms of the energy gaps and image potential states appearing in these surfaces. The calculated distance behaviours of the energy levels corresponding to the first excited (Li-$1s^2 2p$) and the negative (Li-$1s^2 2s^2$) atomic configurations indicate that they can also participate in the ion-surface charge exchange process.

1. Introduction

The understanding of the mechanisms of charge exchange between an atom and a surface occurring either in non-equilibrium processes like ion-surface collisions or in equilibrium processes like adsorption/desorption, is a matter of enormous interest in basic and applied researches such as surface characterization, micro- and nano-technology, film growth, etc. The quite extensively investigated resonant electron tunnelling as one of the most important mechanisms of charge transfer in the interaction of alkali metal ions with metal surfaces is still the object of numerous theoretical and experimental studies [1–22]. In the case of a Li projectile scattered from a metallic surface, its low ionization potential (5.39 eV) when compared with the typical values of metals work functions (ϕ, varies between 4 and 5.5 eV) induces to think in small neutral fractions that should decrease with increasing ϕ, if we see the surface as a jellium. In this surface model the Li level is broadened and shifted by the image potential, remaining above the Fermi level for close distances. For larger values of the metal work function the level crosses above the Fermi level at larger atom surface separations, and the electron capture becomes less efficient. In the description of the Li^+/metal surface collision it is usually assumed a memory loss along the incoming trajectory, and the initial condition for the departure from the surface at a distance typically around 3 a.u. corresponds to the ionic state Li^+. This initial charge state for the outgoing trajectory is consistent with the extended image potential upward shift of the level that positions it well above the Fermi level. In this form it is found a probability of neutralization to the ground state that increases as the Li outgoing energy diminishes, because at low energies the interaction time is large enough as to involve the region of distances for which the Li level is below the Fermi level.

Different theoretical treatments of the dynamical collision process were performed, but in general they consider a level shift only induced by the image potential and Li^+ as the initial condition for the outgoing trajectory. For example, Marston et al. [9] used a generalized time-dependent Anderson–Newns Hamiltonian for describing resonant charge transfer in Li^+/Cu(100) collisions that included electron spin, excited neutrals and negative-ion states. They employed a systematic $1/N$ expansion to treat the many-body correlations, with N the spin degeneracy of the electron; and they extracted the coupling term from the level width calculated by

* Corresponding author. Tel.: +54 342 4559175; fax: +54 342 4550944.
E-mail address: egarcia@intec.unl.edu.ar (E.A. García).

0039-6028/$ - see front matter © 2009 Elsevier B.V. All rights reserved.
doi:10.1016/j.susc.2008.12.022

assuming that the copper is adequately described by a jellium metal.

Niedfeldt et al. [12] used also a time-dependent Anderson Hamiltonian for describing the resonant charge transfer between Li^+ and Al(001) surface within the non-crossing approximation to account for the spin statistics [23]. In this case the coupling parameter was determined from the adsorbate resonance width calculated by using a first-principles periodic density functional theory that is able to include the band structure details. Their theoretical calculation does not allow for extracting easily the level shifts, and therefore they used shifts that essentially follow the classical image potential.

Canario et al. [17] presented experimental and theoretical results of the neutralization of Li^+ ions scattered off a Ag(100) surface. They performed a fully quantum-mechanical treatment based on the wave-packet propagation (WPP) technique by using either a potential that reproduces the main features of the Ag(100) surface (projected bandgap, surface and image potential states), or a free-electron modelling of the Ag(100) surface. The spin statistics effect was accounted for in an approximate way. The authors found that the existence of the projected bandgap produced strong modifications in the adiabatic calculation of the shift and width of the atom level as compared to the free-electron metal case. On the other hand they found that the band structure effects almost disappeared for the moving atom due to the finite interaction time, and that a free-electron model was successful for describing the experimental data in the case of a Li^+/Ag(100) collision. In the adiabatic calculation performed in Ref. [17] the atom level is shifted above the Fermi level at much shorter distances than in the free-electron case; and provided that the impinging Li(2 s) atom is completely ionized in the incoming trajectory, time reversal was used to obtain the neutralization probability of the outgoing Li^+ ion.

An experimental study of the effect of progressive changes in the electronic structure of (111) metal surfaces (Ag, Cu, Au) on neutralization of Li^+ ions revealed an anomalously high neutralization on these high workfunction surfaces and an unusual ion energy dependence [15]. The authors found that in the case of Ag(111) the jellium model underestimated the experimental data although the energy trend was similar. In the case of Cu(111), however, the prediction of this model turned out to be off by a factor of several hundred and did not reproduce the energy dependence. Essentially no neutralization was expected in the case of Au(111) according to the 'traditional' picture of a Li^+ departing from a metal surface of very high work function (5.4 eV). They attributed their results to a non-adiabatic electron transfer process involving a dynamical velocity dependent electron pickup from the surface states and a very large survival due to the presence of the *L*-bandgap in these (111) surfaces. Hamoudi et al. [21] found recently that the neutralization probability of Li^+ on Au(100) had a similar magnitude to that on Au(111) and a similar energy dependence. On the other hand, it is possible to observe that the neutralization probabilities measured in the case of Li^+ scattered by metal surfaces of similar workfunctions (ϕ around 4.6 eV) such as Ag(100) [17], Ag(111) [15], and Cu(100) [16] are also similar in magnitude and dependence on energy. The question is how much the neutralization mechanism depends on the electronic structure of these surfaces related to positions of bandgaps and image potential states [24,25].

The neutral fraction found in the case of Li^+ scattered by a highly oriented pyrolytic (HOPG) graphite surface with ϕ equal to 4.7 eV [26] was also similar to that measured in the Cu (100), Ag (100) and Ag (111) surfaces in the range of large incoming energies. In Ref. [26] a complete opposite picture to the jellium model was used for describing the collision system. The atom-surface interaction model is essentially based on the expansion of the solid state wavefunctions in atomic orbitals centred at the different atoms of the surface, which leads to localized atom–atom interactions weighted by the density matrix elements of the solid that account for the band structure details. The short range chemical interactions between the projectile atom and the surface determine a pronounced downshift of the atom level below the Fermi level at distances close to the surface, thus leading to a practically full neutralization in the incoming path. In this form a neutral atom is leaving the surface and an increasing neutral fraction is expected at larger energies.

We used in the present work the same model calculation of Ref. [26] for describing the resonant neutralization of Li^+ impinging on Cu(100) and Cu(111) for different incident energies. The adiabatic shift and width of the Li(2 s) level and the neutral fraction in the collision process are calculated by using a Green function technique. It is assumed the Li ground state as the only active channel for the neutralization process. A good agreement with the experimental trends is found within the range of not very low exit energies (>600 eV), showing a better agreement in the case of Cu(100) surface. In order to explain the differences between the theoretical and experimental results we discussed the possible effect of the energy gaps and of the image potential states on the neutralization process. It is also discussed the contribution of other electronic channels not considered in this first approximation: neutralization to the excited state Li(1 $s^2$2p) and the formation of negative ions as an intermediary state in the process of neutralization to the ground state.

2. Theory

2.1. Interaction model

The Hamiltonian for describing the atom-surface interaction is an Anderson one like the following:

$$H = \sum_{\vec{k},\sigma} \varepsilon_{\vec{k}} \hat{n}_{\vec{k}\sigma} + H_{atom} + H_{atom-surface} \tag{1}$$

The first term in Eq. (1) refers to the solid states of energy $\varepsilon_{\vec{k}}$ and occupation number $\hat{n}_{\vec{k}\sigma}$ per spin projection σ. The second term is related with the atom electronic configurations considered as the most probable ones in the charge exchange process; and finally the last term is the interaction between these electronic configurations and the band states of the solid surface.

In this work we are considering only the neutralization to the ground state of the Li atom, then the H_{atom} is given by the expression:

$$H_{atom} = E_0|0\rangle\langle 0| + \sum_{\sigma} E_{1/2}|\sigma\rangle\langle\sigma| \tag{2}$$

where $|0\rangle, |\sigma\rangle$ represent the ionic (Li-1s^2) and neutral (Li-1$s^2$2s) configurations, respectively. The two energy degenerate possibilities of spin σ are taken into account in the neutral configuration (1$s^2$2s).

Within the *bond-pair* model used for describing the atom-surface interaction [27], the difference between total energies $E_{1/2} - E_0$ that asymptotically gives the Li ionization energy, results to be:

$$\begin{aligned}\tilde{\varepsilon}_I &= E_{1/2} - E_0 \\ &= \varepsilon_0 - \sum_{\vec{R}_s} V^{Z_s,\vec{R}_s}_{2s,2s} + \sum_{i,\vec{R}_s} (2\tilde{J}_{2s,i\vec{R}_s} - \tilde{J}^X_{2s,i\vec{R}_s})\langle n_i\rangle - \sum_{i,\vec{R}_s} S_{2s,i\vec{R}_s} V^{\dim}_{2s,i\vec{R}_s} \\ &\quad + \frac{1}{4}\sum_{i,R_s} S^2_{2s,i\vec{R}_s} \Delta E_{2s,i\vec{R}_s}\end{aligned} \tag{3}$$

In Eq. (3) the index *i* denotes the type of orbital (s, p, d,...) and $\vec{R}_s$ the position of the atoms in the solid; while *2* s indicates the active

state in the projectile atom. The $\varepsilon_0 - \sum_{\vec{R}_s} V^{Z_s,\vec{R}_s}_{2s,2s}$ term accounts for the one-electron contributions (kinetic energy and electron-nuclei interactions); $\tilde{J}_{2s,i\vec{R}_s}, \tilde{J}^X_{2s,i\vec{R}_s}$ are the direct and exchange Coulomb integrals calculated up to a second order expansion in the overlap $S_{2s,i\vec{R}_s}$ of the symmetric orthogonal atomic basis set. The average occupations $\langle n_i \rangle$ of the atoms in the solid are the non-perturbed ones obtained from the local surface density of states. The $\Delta E_{2s,i\vec{R}_s}$ term corresponds to the difference between the projectile atom and surface atom energy terms, and $V^{\dim}_{2s,i\vec{R}_s}$ is the off-diagonal term that also includes the two-electron contributions to the hopping within a mean-field approximation. The super-index *dim* indicates that it is calculated within the orthogonal basis set for the corresponding dimmer composed by the projectile atom and one of the solid at the position $\vec{R}_s$. The total energies are calculated without allowing charge exchange between atom and surface, being the Li energy level variation caused by overlap and mean-field electrostatic interactions.

This model interaction is fundamentally based on the expansion of the band states $\varphi_{\vec{k}}$ in the atomic orbital basis set $\{\phi_i(\vec{r} - \vec{R}_S)\}$:

$$\varphi_{\vec{k}}(\vec{r}) = \sum_{i,\vec{R}_S} c^{\vec{k}}_{i,\vec{R}_S} \phi_i(\vec{r} - \vec{R}_S), \tag{4}$$

The coefficients $c^{\vec{k}}_{i,\vec{R}_s}$ determine the density matrix elements $\rho_{i,j,\vec{R}_s,\vec{R}_{s'}}(\varepsilon)$ of the solid through the expression (the index *i* and *j* denote the Cu 3d, 4 s and 4p orbitals in the case of the valence band states):

$$\rho_{i,j,\vec{R}_s,\vec{R}_{s'}}(\varepsilon) = \sum_{\vec{k}} c^{\vec{k}*}_{i,\vec{R}_s} c^{\vec{k}}_{j,\vec{R}_{s'}} \delta(\varepsilon - \varepsilon_{\vec{k}}) \tag{5}$$

In this way our model incorporates the localized properties of the involved atoms through an adequate atomic basis set, and the extended properties of the surface from the knowledge of the density matrix elements given by Eq. (5) [27].

The effect of the long range interactions is introduced by considering the image potential defining the behaviour for large normal distances (z) to the surface ($z > z_a$) [27,28]:

$$\varepsilon_I(R) = \begin{cases} \tilde{\varepsilon}_I(R) + V_{im}(z_a) & \text{for } z \leqslant z_a \\ \tilde{\varepsilon}_I(R) + V_{im}(z) & \text{for } z \succ z_a \end{cases} \tag{6}$$

where

$$V_{im}(z) = \frac{1}{4(z - z_{im})}$$

and z_{im} is the image plane distance from the first surface layer of atoms.

Consistently with this picture, the $H_{atom\text{-}surface}$ is:

$$H_{atom\text{-}surface} = \frac{1}{\sqrt{2}} \sum_{\vec{k},\sigma} \left[V_{\vec{k},2s} \hat{c}^+_{\vec{k}\sigma} |0\rangle\langle\sigma| + h.c. \right]$$

in which $1/\sqrt{2}$ has to be with the two–fold spin degeneration, and the coupling term $V_{\vec{k},2s}$ is calculated accordingly to the expansion Eq. (4) as:

$$V_{\vec{k},2s} = \sum_{i,\vec{R}_s} c^{\vec{k}}_{i,\vec{R}_s} V^{\dim}_{2s,i\vec{R}_s} \tag{7}$$

It is important to notice that the inner bands of the surface can be straightforwardly included in our calculation by considering them as zero-width bands.

2.2. Dynamical evolution of the scattering process: atom charge state probabilities

The Green functions required to solve the time evolution introduced by the time dependence of the projectile position respect to the surface $\vec{R} = \vec{R}(t)$, are:

$$\begin{aligned} G_\sigma(t,t') &= i\Theta(t'-t)\langle\Phi_0|\{|\sigma\rangle\langle 0|_{t'}, |0\rangle\langle\sigma|_t\}|\Phi_0\rangle \\ F_\sigma(t,t') &= i\langle\Phi_0|[|\sigma\rangle\langle 0|_{t'}, |0\rangle\langle\sigma|_t]|\Phi_0\rangle \end{aligned} \tag{8}$$

being Φ_0 the wave function that describes the interacting system in the Heisenberg scheme. These Green functions are calculated by using the equations of motion (EOM) method solved up to a second order in the coupling parameter which has proved to be a very accurate calculation of time dependent processes [29].

After some algebra, and taking into account the norm constraint:

$$|0\rangle\langle 0| + \sum_\sigma |\sigma\rangle\langle\sigma| = 1$$

the final differential equations obtained are ($\tilde{V}_{\alpha,2s} = V_{\alpha,2s}/\sqrt{2}$):

$$\begin{aligned} i\frac{d}{dt}G_\sigma(t,t') &= (1 - \langle|-\sigma\rangle\langle-\sigma|\rangle_{t'})\delta(t-t') + \varepsilon_I G_\sigma(t,t') \\ &\quad - i\sum_k \tilde{V}^*_{k,2s}(t)\langle|-\sigma\rangle\langle 0|\hat{c}_{k-\sigma}\rangle_{t'} e^{-i\varepsilon_k(t-t')} \\ &\quad + \int_t^{t'} d\tau \Sigma^A_\sigma(t,\tau) G_\sigma(\tau,t') \end{aligned} \tag{9}$$

$$\begin{aligned} i\frac{d}{dt}F_\sigma(t,t') &= \varepsilon_I F_\sigma(t,t') - i\sum_k (2f(\varepsilon_k) - 1)\tilde{V}^*_{k,2s}(t) \\ &\quad \times \langle|-\sigma\rangle\langle 0|\hat{c}_{k-\sigma}\rangle_{t'} e^{-i\varepsilon_k(t-t')} + \int_{t_0}^{t} d\tau \Sigma^R_\sigma(t,\tau) F_\sigma(\tau,t') \\ &\quad + \int_{t_0}^{t'} d\tau \Omega_\sigma(t,\tau) G_\sigma(\tau,t') \end{aligned} \tag{10}$$

where:

$$\begin{aligned} \langle|\sigma\rangle\langle 0|\hat{c}_{\vec{k}\sigma}\rangle_t &= \sum_{i,\vec{R}_s} c^{\vec{k}}_{i,\vec{R}_s}(-1/2)\int_{t_0}^{t} d\tau \tilde{V}_{i\vec{R}_s,2s}(\tau) e^{i\varepsilon_{\vec{k}}(\tau-t)}[F_\sigma(\tau,t) \\ &\quad - (2f(\varepsilon_{\vec{k}}) - 1)G_\sigma(\tau,t)] \end{aligned} \tag{11}$$

The self-energies determining the motion equations of these Green functions read:

$$\begin{aligned} \Sigma^A_\sigma(t,\tau) &= i\Theta(\tau - t)\sum_{i,j,\vec{R}_s,\vec{R}_{s'}} \tilde{V}^*_{i\vec{R}_s,2s}(t)\tilde{V}_{j\vec{R}_{s'},2s}(\tau)\int_{-\infty}^{\infty} d\varepsilon \rho_{i,j,\vec{R}_s,\vec{R}_{s'}}(\varepsilon) \\ &\quad \times [1 + f(\varepsilon)]e^{i\varepsilon(\tau-t)} \\ &= \Sigma^{R^*}_\sigma(\tau,t) \end{aligned} \tag{12}$$

$$\begin{aligned} \Omega_\sigma(t,\tau) &= i\sum_{i,j,\vec{R}_s,\vec{R}_{s'}} \tilde{V}^*_{i\vec{R}_s,2s}(t)\tilde{V}_{j\vec{R}_{s'},2s}(\tau)\int_{-\infty}^{\infty} d\varepsilon \rho_{i,j,\vec{R}_s,\vec{R}_{s'}}(\varepsilon)[2f(\varepsilon) - 1] \\ &\quad \times [1 + f(\varepsilon)]e^{i\varepsilon(\tau-t)} \end{aligned} \tag{13}$$

$f(\varepsilon)$ is the Fermi-Dirac function, $f(\varepsilon) = 1/[1 + e^{(\varepsilon-\mu)/k_BT}]$.

Adequate boundary conditions are required for solving Eq.(10). They are in the case of $Li^+ \rightarrow Li^0$:

$$\langle|\sigma\rangle\langle\sigma|\rangle_{t_0} = \langle|-\sigma\rangle\langle-\sigma|\rangle_{t_0} = 0 \quad \text{and} \quad F_\sigma(t_0,t') = -G_\sigma(t_0,t'),$$

while in the case of $Li^0 \rightarrow Li^+$:

$$\langle|\sigma\rangle\langle\sigma|\rangle_{t_0} = \langle|-\sigma\rangle\langle-\sigma|\rangle_{t_0} = \frac{1}{2} \quad \text{and} \quad F_\sigma(t_0,t') = G_\sigma(t_0,t').$$

In this way, we calculated $\langle\hat{n}_\sigma\rangle = \langle|\sigma\rangle\langle\sigma|\rangle$ from its time derivative:

$$\frac{d}{dt}\langle\hat{n}_\sigma\rangle = 2\mathrm{Im}\sum_{\vec{k}} \tilde{V}_{\vec{k},2s}(t)\langle|\sigma\rangle\langle 0|\hat{c}_{\vec{k}\sigma}\rangle_t$$

By using equations Eqs. (11) and (7) and the expression Eq. (5) of the density matrix elements, we arrived to:

$$\frac{d}{dt}\langle\hat{n}_\sigma\rangle = -2\mathrm{Im}\sum_{i,j,\vec{R}_s,\vec{R}_{s'}}\int_{-\infty}^{\infty} d\varepsilon \rho_{i,j,\vec{R}_s,\vec{R}_{s'}}(\varepsilon)\tilde{V}^*_{2s,i\vec{R}_s}(t) \times \int_{t_0}^{t} d\tau \tilde{V}_{2s,j\vec{R}_{s'}}(\tau)e^{i\varepsilon(\tau-t)}[F_\sigma(\tau,t)-(2f(\varepsilon)-1)G_\sigma(\tau,t)] \quad (14)$$

The probability of having neutral Li atoms in the ground state is finally $P^0_{res} = 2\langle\hat{n}_\sigma\rangle$.

2.3. Energy level width and shift due to the adiabatic interaction

Our model allows for calculating the shift and the width of the energy level of an atom interacting in an adiabatic way with the surface [30]. In this case the Fourier transform of the Green function $G_\sigma(t,t')$ defined by the differential Eq. (9) is:

$$G_\sigma(\omega) = \frac{1-\langle\hat{n}_\sigma\rangle - \sum_{\vec{k}}\frac{\tilde{V}^*_{\vec{k},2s}}{\omega-\varepsilon_{\vec{k}}-i\eta}\langle|\sigma\rangle\langle 0|\hat{c}_{\vec{k}\sigma}\rangle}{\omega-\varepsilon_I-\Sigma^A_\sigma(\omega),}$$

The level width Γ as a function of the atom position $\vec{R}$ respect to the surface is defined by the imaginary part of $\Sigma^A_\sigma(\omega)$ evaluated at the atom energy level shifted by the interaction ($\bar{\varepsilon}_I$):

$$\Gamma = 2\mathrm{Im}\Sigma^A_\sigma(\bar{\varepsilon}_I) = 2\pi\sum_{i,j,\vec{R}_s,\vec{R}_{s'}}\tilde{V}'_{i\vec{R}_s,2s}(\vec{R})\tilde{V}_{j\vec{R}_{s'},2s}(\vec{R})\rho_{i,j,\vec{R}_s,\vec{R}_{s'}}(\bar{\varepsilon}_I)[1+f(\bar{\varepsilon}_I)] \quad (15)$$

The atom energy level shift is given by the real part of $\Sigma^A_\sigma(\omega)$, being $\bar{\varepsilon}_I$ defined as:

$$\bar{\varepsilon}_I = \varepsilon_I + \frac{P}{\pi}\int_{-\infty}^{\infty} d\varepsilon \frac{\mathrm{Im}\Sigma^A_\sigma(\varepsilon)}{\varepsilon_I-\varepsilon} \quad (16)$$

where P denotes the principal value.

The projected density of states per spin on the Li atom, $\rho_\sigma = (1/\pi)\ \mathrm{Im}\ G_\sigma(\omega)$, can be also calculated in this form at different distances between Li atom and Cu surface.

The density matrix elements defined by Eq. (5) can be written by discriminating between the parallel ($\vec{k}_\parallel$) and perpendicular (k_z) to the surface components of the wavevector $\vec{k} = (\vec{k}_\parallel, k_z)$, as:

$$\rho_{i,j,\vec{R}_s,\vec{R}_{s'}}(\varepsilon) = \sum_{\vec{k}_\parallel,k_z} c^{\vec{k}_\parallel}_{i,\vec{R}_s}(k_z)c^{\vec{k}_\parallel}_{j,\vec{R}_{s'}}(k_z)\exp[-i\vec{k}_\parallel.(\vec{R}_s-\vec{R}_{s'})]\delta(\varepsilon-\varepsilon_{\vec{k}_\parallel,k_z}) \quad (17)$$

The contributions from site diagonal and non-diagonal terms of the matrix density to the level width Γ can be separated in Eq. (15) accordingly with Eq. (17), being obtained the following expression:

$$\frac{\Gamma}{2\pi} = \sum_{i,j,\vec{R}_s}\tilde{V}^*_{i\vec{R}_s,2s}(\vec{R})\tilde{V}_{j\vec{R}_s,2s}(\vec{R})\rho_{i,j,\vec{R}_s}(\bar{\varepsilon}_I)[1+f(\bar{\varepsilon}_I)] + \sum_{i,j,\vec{R}_s\neq\vec{R}_{s'}}\tilde{V}^*_{i\vec{R}_s,2s}(\vec{R})\tilde{V}_{j\vec{R}_{s'},2s}(\vec{R})\sum_{\vec{k}_\parallel,k_z}c^{\vec{k}_\parallel}_{i,\vec{R}_s}(k_z)c^{\vec{k}_\parallel}_{j,\vec{R}_{s'}}(k_z) \times \exp[-i\vec{k}_\parallel.(\vec{R}_s-\vec{R}_{s'})]\delta(\bar{\varepsilon}_I-\varepsilon_{\vec{k}_\parallel,k_z})[1+f(\bar{\varepsilon}_I)] \quad (18)$$

The main contribution is provided by the first term which involves only the local and partial density of states (LDOS) of the surface:

$$\rho_{i,j,\vec{R}_s}(\varepsilon) = \sum_{\vec{k}_\parallel,k_z}c^{\vec{k}_\parallel}_{i,\vec{R}_s}(k_z)c^{\vec{k}_\parallel}_{j,\vec{R}_s}(k_z)\delta(\varepsilon-\varepsilon_{\vec{k}_\parallel,k_z}) \quad (19)$$

The second term in Eq. (18), $\vec{R}_s \neq \vec{R}_{s'}$, accounts for the peculiarities of the 3D band structure of a crystalline target, that can be for instance the existence of a band gap along certain directions.

In this work the self-energies for the dynamical process given by Eqs. (12) and (13), and the level width and shift for the static situation, Eqs. (15) and (16), were calculated by considering only the site diagonal terms of the density matrix, that is the LDOS $\rho_{i,j,\vec{R}_s}(\varepsilon)$ [26,28]. In this way the extended features of the surface states actually involved in our calculation are those described by the LDOS for both Cu surfaces. This is expected to be a good approximation for large angle collisions and not very low impinging energies in which the time spent by the projectile near the surface is very short to capture the finest structure characteristics along the parallel direction to the surface.

3. Results and discussion

3.1. Dependence of the Li ionization energy level with the distance to the surface

The Li ionization energy level was calculated from Eqs. (3) and (6) by using a full-electron description of the Li–Cu interacting system, with atomic Gaussian basis set provided by Huzinaga [31]. In both Li and Cu atoms, p-polarization functions were included. The image plane position z_{im} is assumed as half an interlayer spacing, 1.71 and 1.97 a.u. for Cu(100) and Cu(111) surfaces, respectively [32], and the matching between the short and long range behaviours of the interaction potential is done at $z_a = 8$ a.u. [27,28]. The local and partial density of states $\rho_{i,j,R_s}(\varepsilon)$ for both Cu surfaces was calculated by using the FIREBALL code [33]. This code is based on a density functional theory within a local density approximation that employs a localized numeric-like orbital basis set [33].

The energy level as a function of the distance to the surface (z), given by Eq. (3), for the Li atom in front of Cu(100) is depicted in Fig. 1a, and for the Li atom in front of Cu(111) in Fig. 1b (the zero energy corresponds to the Fermi level in each case). This energy level value does not include the shift introduced by the atom-surface coupling terms in the interaction process.

In Fig. 1 it is also shown the local density of states projected on one surface atom, calculated as:

$$\rho_{\vec{R}_s}(\varepsilon) = \sum_{i,j=3d,4s,4p}\sum_{\vec{k}_\parallel,k_z}c^{\vec{k}_\parallel}_{i,\vec{R}_s}(k_z)c^{\vec{k}_\parallel}_{j,\vec{R}_s}(k_z)\delta(\varepsilon-\varepsilon_{\vec{k}_\parallel,k_z})$$

In both Cu surfaces the 3d-orbitals contribute strongly to the peaked structure in the LDOS, being this one closer to the Fermi level in the Cu (100) case. The 4 s and 4p valence states are mainly contributing to the conduction band.

The distance dependence of the Li ionization level was calculated by assuming in Eq. (3) the interaction with: (i) only the scatter atom on the surface at $R_s = (0,0,0)$; (ii) the scatter atom and its first neighbors; and (iii) the scatter atom and its first and second neighbors. We can observe that there are not important changes when second neighbors are added, and that the downshift of the energy level close to the surface becomes more pronounced when there are included all the surface atoms that are able of interacting with the projectile atom. A less marked opposite effect is observed at large distances. The image potential is practically the only one responsible of the energy shift of the Li ionization level (5.39 eV) at distances larger than 9 a.u. It is observed in Fig. 1 that the ionization level is crossing below the Fermi level at distances around 10 a.u. in the case of the smallest work function Cu(100) surface ($\phi = 4.6$ eV), while in the case of Cu(111) ($\phi = 4.95$ eV), it is above the Fermi level up to distances around 12 a.u.. The interaction is operative up to distances around 10 a.u accordingly to the distance dependence of the hopping integrals.

It is possible to infer about the resonant neutralization probability by analyzing the energy level position in comparison with the

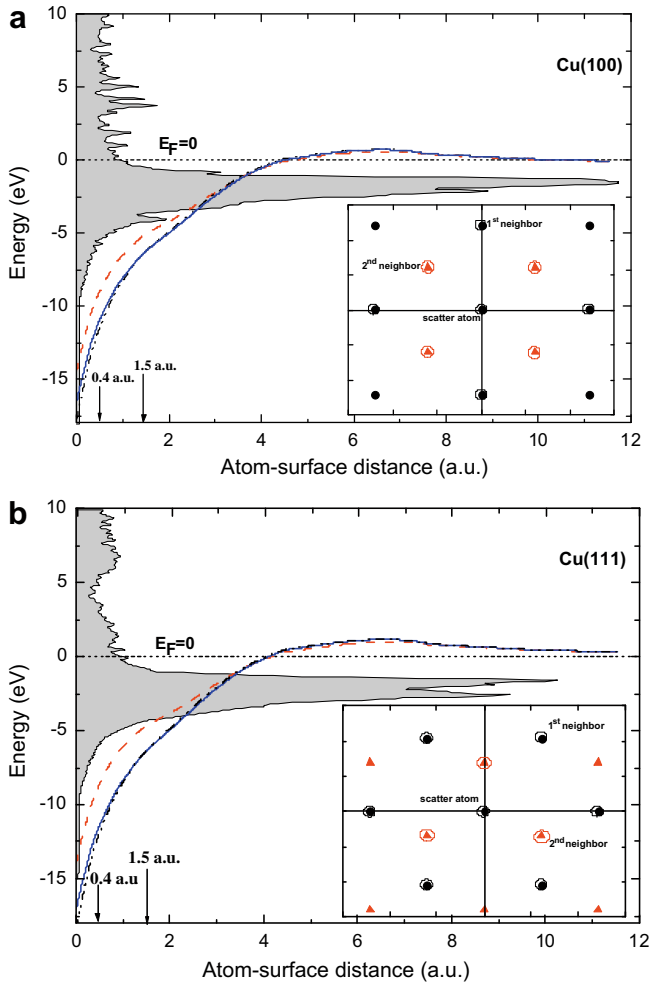

Fig. 1. Distance dependence of the Li ionization energy level. (a) Cu(1 0 0): when the interaction with only the scatter atom is considered (dash line); including the first-neighbors (solid line); including the first and second-neighbors (dash–dot–dot line). (b) Cu(1 1 1): the same as for Cu(1 0 0) surface case. The shadowed area corresponds to the Cu surface LDOS. In the inset the scatter atom and its first and second neighbors on the surface plane are shown.

density of occupied and empty band states of the surface. Within the incoming trajectory the Li^+ ion is going to be neutralized efficiently due to the pronounced downshift of its energy level close to the turning point, whose minimum (0.4 a.u.) and maximum (1.5 a.u.) values within the energy range analyzed are indicated in Fig. 1. Along the outgoing trajectory the electron loss process is more probable in the case of Cu (1 1 1) because the energy level crosses above the Fermi energy at smaller distance from the surface and becomes more upward shifted. But due to the atom energy level position above the Fermi energy for large operative distances, a decaying neutral atom surviving probability is expected for both surfaces at low incoming energies.

Regarding the shift of the energy levels of an atom in front of a metallic surface, there are theoretical and experimental predictions that this shift can be substantially modified at smaller distances compared to the image potential [34–37,26]. It is found that close to the surface strong short-range *chemical* interactions with neighboring metal atoms become important and lead to large shifts in the energy levels, and that ion neutralization at clean, high-work function metal surfaces occurs at much smaller ion-surface separations, typically 2–3 a.u., than inferred from earlier measurements [35].

3.2. Dynamic collision process: neutralization probability. Atom level shift and width due to the adiabatic interaction

The measurements of Ref. [15,16] were performed by using a scattering angle δ of 114° and an exit angle normal to the surface ($\beta = 90°$), this means an incident angle $\alpha = 24°$ respect to the surface plane. To include all the Cu atoms of the surface that are able to interact with the projectile atom, according to the experimental scattering geometry, becomes a very hard task due to the complexity of the Li–Cu system. Preliminary calculations by considering only the scatter atom on the surface and either the experimental scattering geometry ($\alpha = 24°$ and $\beta = 90°$), or a normal trajectory ($\alpha = \beta = 90°$) but with incoming and exit velocity values corresponding to the perpendicular components of the experimental geometry, lead to the same results. This fact suggested that the exchange process is defined fundamentally along the outgoing trajectory. On the other hand, minor differences were found between the final neutralization probabilities calculated by considering either incoming neutral atoms or incoming ions, confirming in this way the memory loss of the incoming trajectory.

Then, our results were obtained assuming a normal trajectory with the corresponding normal component of the incoming energy $E_{in} = E_k^* \sin^2 24°$ and an exit energy $E_{out} = 0.7^* E_k$, being E_k the incoming ion kinetic energy and 0.7 the energy loss factor for the Li–Cu system at a scattering angle of 114°. The distance of closest approach at the different incoming energies is calculated consistently with the binary collision model from the interaction energy of the dimmer Li–Cu system.

Taking into account the convergence with neighbor atoms found in the case of the Li energy level calculation (Fig. 1), the scatter Cu atom and its first neighbors were also considered in the description of the dynamical interaction process (the sum over R_s in Eq. (12) and (13) is extended to the scatter atom and its first neighbors). The Cu-3s and Cu-3p inner band states were also included in the calculation.

It is not expected in this case parallel velocity effects [1,38–39] due to the outgoing motion of the projectile perpendicular to the surface.

The neutralization probability as a function of the Li ion distance to the surface is shown in Fig. 2, for the two Cu surfaces and for two exit energy values: 300 and 1200 eV. These results can be well understood if the adiabatic evolution of the charge exchange process by considering both, the shift and the width of the energy level due to the interaction, is simultaneously observed. Then, in Fig. 2a and b the energy level shifted accordingly to the expression Eq. (16), and the width calculated by using Eq. (15) drawn as error bars are also shown. Starting from a highly neutralized Li ion at the beginning of the outgoing path, the upward shift of the projectile level above the Fermi energy with a level width giving place only to electron loss processes, occurs at smaller distances in the case of Cu(1 1 1). Thus, it becomes evident from these figures that the neutralized Li is going to survive more efficiently in the Cu(1 0 0) surface for finite interaction times.

It is interesting to compare (see Fig. 3) the large distance ($z > 6$ a.u.) behaviour of the level width calculated by using Eq. (15) with the level width obtained from the projected density of states calculated using a first principles electronic structure method [13]. A periodic density functional theory (DFT) within a local density approximation (LDA) is used in the calculation of Ref. [13] in order to investigate the effects of a Cu surface band gap on the Li ionization level lifetime. They found that the d-band can mediate an effective interaction between the energy levels of the adsorbate resulting in a hybridization of the Li 2 s and 2p orbital [14]. In consequence they have also performed a rough estimate of the adiabatic width of the sp-hybridized Li level [13,14]. In Fig. 3 their results by either considering or not the sp-hybridization are shown.

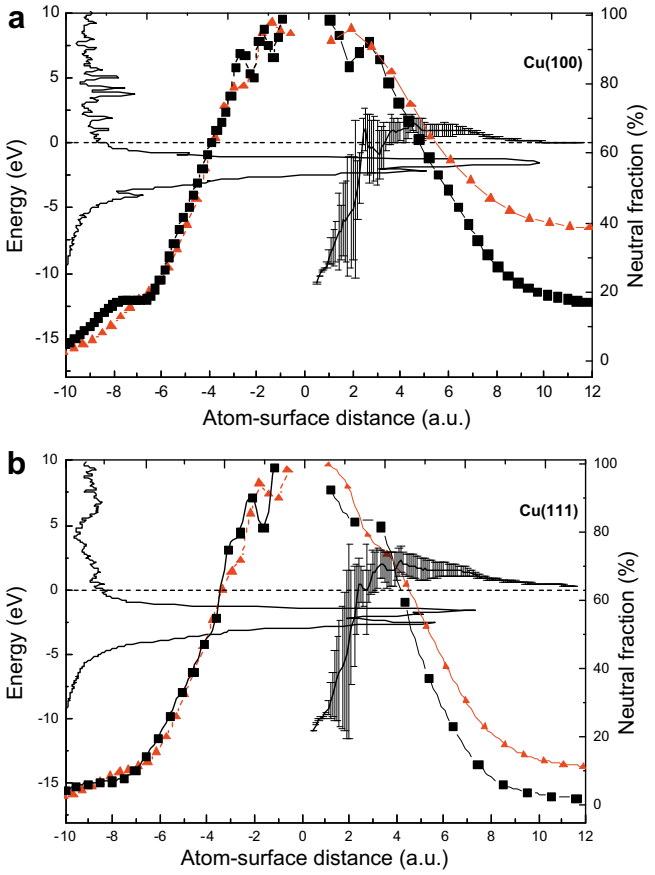

Fig. 2. Evolution of the calculated neutral fraction along the trajectory for (a) Cu (100) and (b) Cu(111) (negative distance represents the incoming path). Square symbols correspond to exit energy equal to 300 eV and the triangles to 1200 eV. The dash-line indicates the Fermi energy level and the LDOS of the Cu surface is also drawn. The energy level shifted accordingly to Eq. (16) a function of the distance along the outgoing path is indicated by a solid line and the level width given by Eq. (15) error bars.

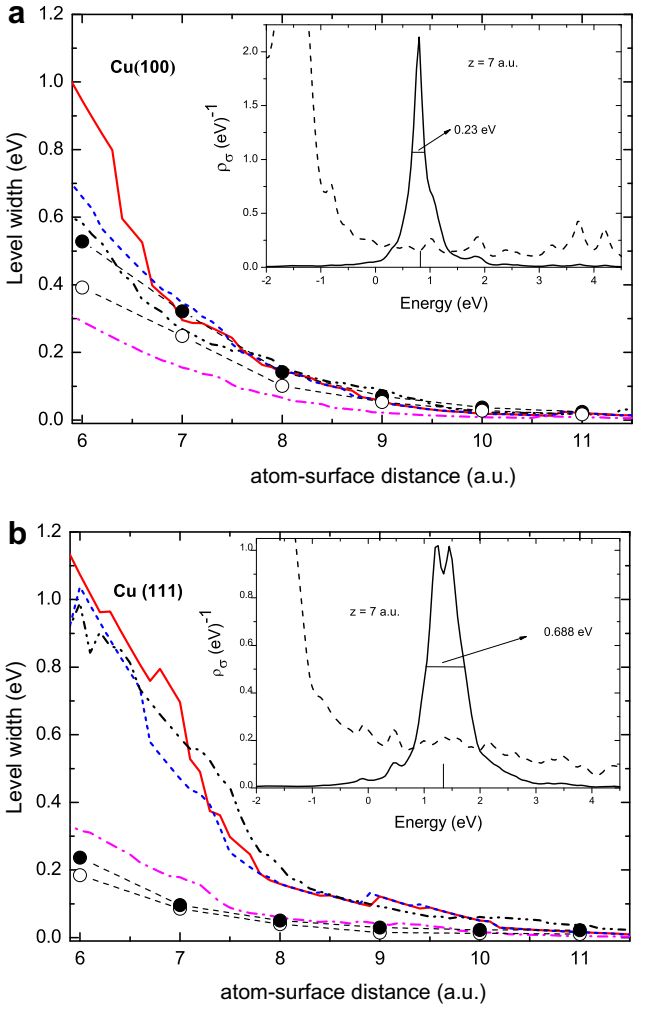

Fig. 3. The behaviour of the energy level width for large distances from the surface: (a) Cu(100) and (b) Cu(111). (i)-Solid line: the calculation including up to the first neighbors and by using 2s and 2p states on Li atom; (ii)-short dash line: the same as (i) but using only a 2s state on Li; (iii)-dash–dot–dot line: the same as (i) but neglecting the interaction with inner bands of Cu; (iv)-dash–dot line: the calculation considering only the scatter atom on the surface. In the inset, the LDOS projected on the Li atom (solid line) and the LDOS of the Cu surface (dash line) are shown. The full and empty circle symbols correspond to the results of Ref. [14], by including and not the 2s–2p Li states mixing, respectively.

In our case the level width calculation is based on the *bond-pair* model of the atom-surface interaction previously developed to study chemisorption's problems [27]. As it is clear from Eq. (18), localized properties of the interacting atoms are taken into account by the atom–atom hopping integrals $\tilde{V}_{jR_s,2s}(R)$, while the surface density of states $\rho_{i,jR_s}(\varepsilon)$ accounts for the extended features of the solid states. It is possible in our model to isolate the different components considered in the calculation of the level width and to analyze their effect from the comparison with the complete calculation. This is the motive of presenting also in Fig. 3 the following calculation options: the level width calculated by considering an extended 2 s and 2p Li basis set but (i) assuming only the interaction with the scatter atom, and (ii) neglecting the interaction with the inner solid band states. Finally, the effect of considering only a 2 s orbital on the Li atom can be also observed from this figure. In our case the inclusion of a Li 2p state introduces changes only due to the symmetric orthogonalization involved in the *bond-pair* model [27]; it is clear from Eq. (2) that the 2p state is not active in the interaction with the surface.

We can observe from Fig. 3 that the contribution arising from all the surface atoms interacting with the adsorbate is the most important in the whole distance range analyzed. The other isolated contributions become significant at smaller distances ($z < 8$ a.u.).

For the Cu(100) surface it is found a good agreement between our results and those from Ref. [14] that include the 2 s–2p hybridization for distances equal or larger than 7 a.u., while for smaller distances our calculation gives larger width values. For the Cu(1 1 1) surface, our calculated level widths are greater than the ones from Ref. [13] in practically the whole range of distances. The level width in our case is very close to the roughly estimated resonance peak width of the projected density of states on the Li atom calculated as $\rho_\sigma = \mathrm{Im}G_\sigma(\omega)/\pi$. In the inset of Fig. 3, ρ_σ is shown for a distance of 7 a.u.

The smaller level width found in Ref. [13] for Cu(111) compared with the one in Cu(100), is explained by the presence of surface band gaps and the energy positions of Li 2 s and 2p levels that lie within the *L*-bandgap of the (111) surface, while they are practically out of the *X*-bandgap of the (100) surface. Therefore, it is expected energy level widths narrower for Li above Cu(111) than above Cu(100) due to the lack of resonant metallic states for the Cu(111) surface. In our calculation it is not taken into account the presence of surface bandgaps because we have considered only site diagonal terms in Eq. (18). This could be a reason of the larger level widths in our case compared with the ones calculated in Ref. [13].

The evolution of the shifted energy level and its width shown in Fig. 2 lead to the conclusion that the Li^+ neutralization probability in Cu(100) is larger than in Cu(111). It is also possible to calculate the static Li 2s occupation in the ground state of the Cu–Li interacting system. For distances smaller than 2.5 a.u., the Li 2s state is totally occupied, for larger distances its occupation decreases. For instance, at $z = 6$ a.u. the adiabatic Li 2 s occupation is 0.16 in Cu(100) and 0.12 in Cu(111). From the point of view of an alkali atom adsorption process, our static calculation gives a shifted energy level due to the interaction equal to 2 eV at 4 a.u. of distance to the Cu(111) surface (see Fig. 2b). This energy value is very similar to the binding energy of the antibonding resonance (AR) measured and calculated in Ref. [40] for the same system at the adsorption distance from the surface layer $R_{ads} = 4$ a.u. The level width is larger in our case leading to a Li atom adiabatic occupation at this distance around 0.3. This means that the adsorption is not totally ionic for small alkali atoms as it was suggested in Ref. [41]. In the case of Cs its lower ionization potential (3.89 eV) and its larger effective interaction distances make more plausible a ground state corresponding to Cu^-+Cs^+ [13].

The projectile atom velocity is regulating the interaction time with the surface. From a practically initial neutral Li atom in the outgoing trajectory (see Fig. 2), a larger normal component of velocity means a smaller interaction time, a lower chance of charge exchange and therefore a larger probability of surviving as a neutral particle as it moves out of the surface. At lower normal velocities regions more distant from the surface become more important for defining the final charge state of the projectile atom. In this case, the asymptotic energy position of the projectile level respect to the Fermi energy allows us to predict a decaying neutral fraction probability for diminishing outgoing energy.

To consider other z_{im} values given in the literature [25], for instance 2.22 a.u. for the two Cu surfaces, does not change qualitatively our results. It is also found that the magnitude and behaviour of the neutralization probability do not depend strongly on the distance of closest approach, particularly at the lowest kinetic energies where the region of large distances to the surface is determining the projectile charge state.

The calculated neutral fractions $P^0_{\mathrm{res}} = 2\langle \hat{n}_\sigma \rangle$ as a function of the exit energy are shown in Fig. 4 for both Cu surfaces.

The experimental results of Ref. [15] and [16] are also shown in this figure. A general increasing trend of neutral fractions for both, high and low incoming energies is measured, and also a marked difference between Cu(100) and Cu(111) surfaces that can not be described satisfactorily by the jellium model as it can be seen also in this figure. For large energies a good agreement between our calculations and the experimental trends ($E_{k,out} > 600$ eV) is observed, while an opposite behaviour is evident for lower energies. In both, Cu(100) and Cu(111) surfaces, the theoretical neutralization probability diminishes with decreasing exit (incoming) energy. In the same figure we included the neutral fraction results obtained by neglecting the spin (spin-less approximation), as to quantify the spin statistical effect in the calculation of the neutralization probability when two spin degenerate states are possible. We can observe that the correct calculation may compare either better or worse than the spin-less one with the experimental trends, depending on the Cu face. But the important conclusion is that the electronic correlation effects associated to the spin degeneration have to be taken into account in this kind of exchange processes.

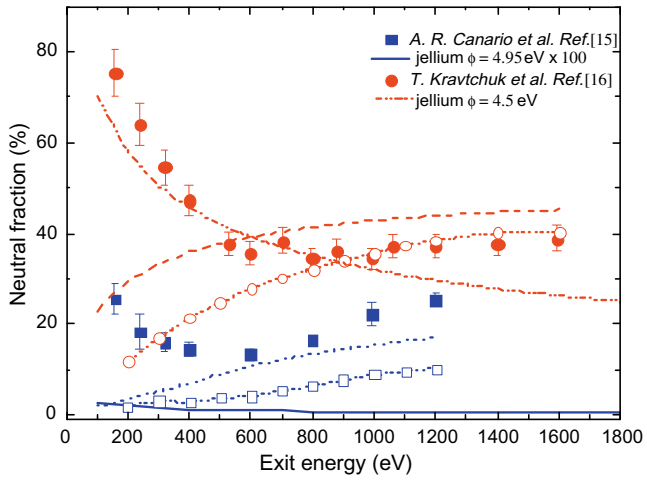

Fig. 4. Theoretical and experimental Li neutral fractions as a function of exit energy for Cu(100) (open and close circles, respectively) and for Cu(111) (open and close squares, respectively). The theoretical neutral fractions calculated by neglecting the spin are included: dash line in the Cu(100) case, and dot line in Cu(111) case. The neutral fractions predicted by the jellium model are also indicated for Cu(100) Ref. [16] (dash-dot-dot line), and for Cu(111) Ref. [15] (solid line).

The pronounced downshift of the Li ionization level due to the short-range interactions with the atoms of the surface is the main responsible of a resonant neutralization that can describe satisfactorily the experimental trends of the neutral fraction for not very low exit energies in both Cu surfaces.

The presence of *L*-bandgaps is expected to increase the neutralization probability due to the blocking of electron loss processes in the Cu(111) surface where the Li 2s level is within the surface bandgap for distances larger than 4 a.u., as it is shown in Fig. 5b. The neglecting of the non-diagonal site terms in the density matrix given by Eq. (17) whoce main contribution is provided by $\vec{k}_{\parallel} = 0$, can be the reason of the underestimation of the experimental results by our theory in the (111) surface.

Nevertheless, the marked increase of the neutral fraction for low energy values observed in the case of Cu(100) [16], which is also observed for the (100) and (111) surfaces of Ag [15,17], can not be attributed to the same reason because of the energy position of the Li ionization level out of the surface bandgap (Fig. 5a). The common and striking feature of these surfaces is the presence of the first ($n = 1$) image potential state (IS) lying inside the energy gap as it can be seen from Fig. 5a. The image potential states are generated by a potential well formed by the Coulomb-like attractive image potential barrier and the repulsive surface barrier [24,25], and they are localized mostly in the vacuum region of metal surfaces beyond the image plane position. It is a difference with the typical surface states (SS) that are localized very close to the surface. A bonding interaction with this image potential state (IS) can shift the Li 2 s level below the Fermi level at distances shorter than 10 a.u., leading in this way to a growing neutralization probability at low energies. This bonding interaction is going to be effective beyond the image plane position where the image potential state is localized, and low exit energies are required to have the time necessary to form this bonding state and take into account its effect on the neutralization process. Thus we can arrive to the following important conclusions. Our model calculation accounts for the short range interactions that allow for a good description of the large energy behaviour of neutralization processes in the case of a projectile of low ionization energy as Li^+ in front of surfaces such as Cu (100). But in the range of low energy collisions a more detailed calculation of the long range interaction effects is required to account for image potential states which can justify a dramatic increase of the neutralization probability due to the down shift of the projectile atom level caused by a bonding interaction. To take into account at large distances only the usual energy level shift by the image potential considered in Eq. (6) seems to be not enough at low exit energies for projectile atoms with ionization energies close to the surface Fermi level. A future improvement of our model may be, in a consistent way with the presence of

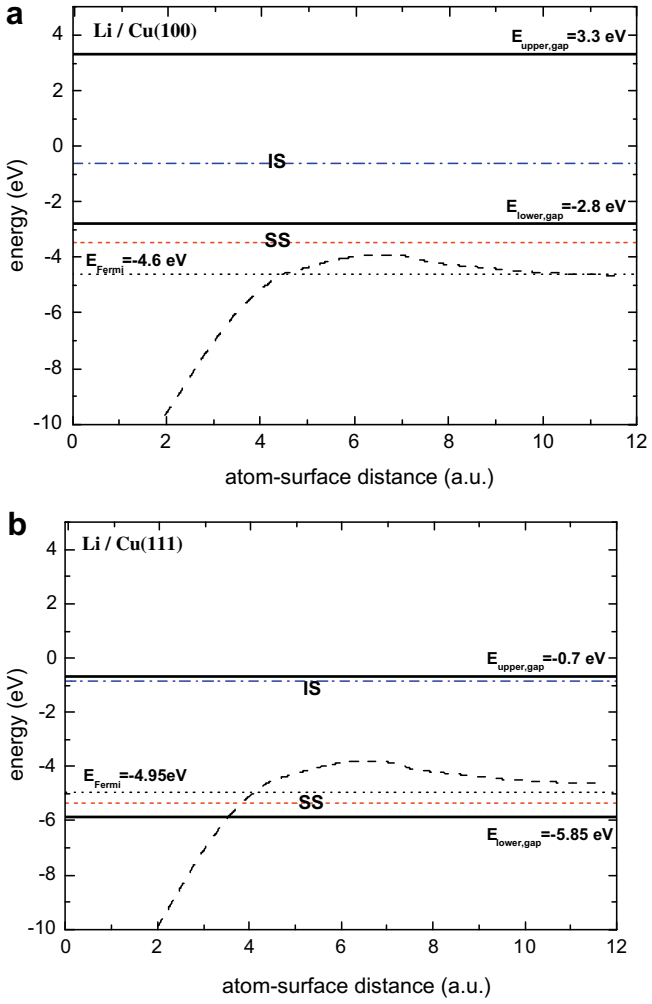

Fig. 5. Li ionization level as a function of the distance to the surface (dashed line). The horizontal lines indicate the energy position of: lower and upper edges of the energy gap (solid lines); image potential state $n = 1$ (dash–dot line); surface state (short dash line); Fermi level (dot line). These values are given relative to the vacuum level $E_V = 0$, and were obtained from Ref. [25]. (a) Cu(100); (b) Cu(111).

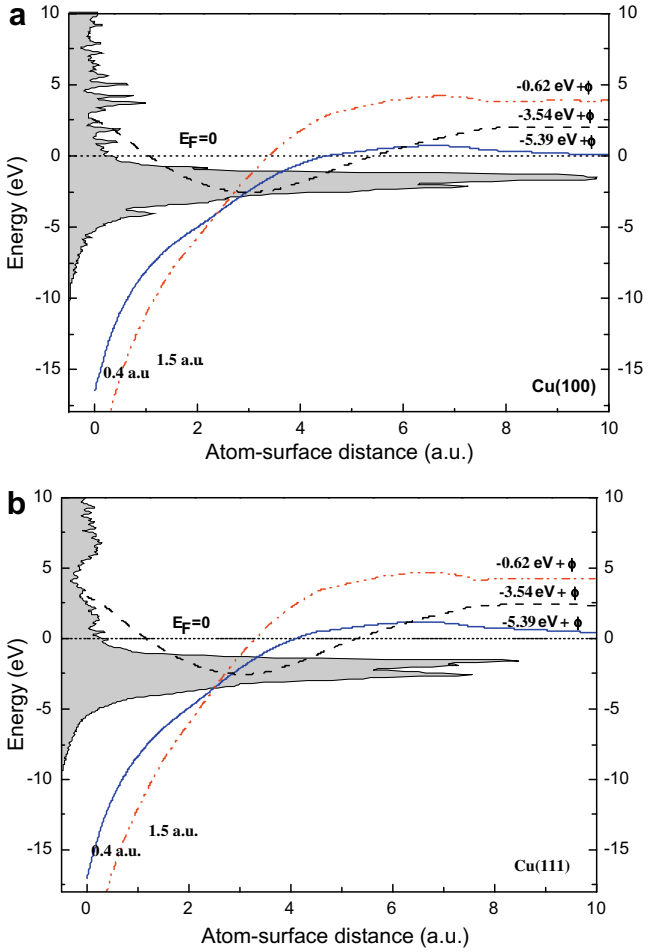

Fig. 6. Evolution of the Li ionization level (solid line), the affinity level (dash–dot–dot line) and the Li-2p excited state (dash line) along the ion trajectory. The corresponding asymptotic values are indicated, being ϕ the Cu work function. The shadowed area corresponds to the Cu LDOS. (a) Cu(100); (b) Cu(111).

localized image potential states, to include the modified potential used by Chulkov et al. [25] This potential reproduces the correct asymptotic behaviour of the image potential beyond the image plane position.

The importance of other possible charge state configurations in the interaction of Li with a surface has been discussed before in previous works. [9,26] There are experimental evidence of excited neutral Li atoms ($1s^2 2p$) in Li^+/Cu(001) collisions through the observed optical transition $2p \rightarrow 2s$ [9]. The energy corresponding to the Li 2p level was calculated as the difference between the total energies of the Li($1s^2 2p$)/Cu and the Li($1s^2$)/Cu systems (by using Eq. (3) with 2p as the active state in the projectile atom). It is shown in Fig. 6 for both Cu surfaces as a function of the distance between the Li atom and the Cu surface. From the energy variation of the Li 2p level, we can expect significant differences between the neutral fractions for large and small kinetic energy values. At large energy values (means small turning point values), electron loss processes are more probable close to the surface during the incoming and exit trajectories due to the upward shift of the 2p energy level. While for small values of the projectile energy, electron capture processes dominate the charge transfer close to the surface. In this way one can conclude that the population of the excited state is going to be more important for low kinetic energies. But in this simple picture we are disregarding the interference between the two correlated neutralization channels (the ground and excited states of Li), which can change significantly the neutralization probability to the ground state obtained when the excited state is not considered [42].

The affinity level calculated as the difference between the total energy of Li($1s^2 2s^2$)/Cu and the total energy of Li($1s^2 2s^1$)/Cu is also included in Fig. 6. The energy downshift suggests that it can also be necessary to take into account the negative Li ion formation ($Li^0 \rightarrow Li^- \rightarrow Li^0$) as an intermediary process contributing to the final neutral fraction.

The ground state neutralization by the Auger mechanism is not possible for low energies because the requirement $I \geqslant 2\,\phi$ (where I *is* the ionization energy) is not accomplished for kinetic energies lower than 600 eV (distance of closest approach larger than 0.75 a.u.).

A calculation including not only the Li ground state, but also the excited and negative charge states in the dynamic evolution of the interacting system, is desirable but very complex computationally.

4. Conclusions

In this work we performed a time-dependent quantum mechanical calculation of the resonant neutralization probability to the ground state of Li^+ impinging on Cu(100) and Cu(111) for

different incident energies. The correct spin degeneration was included in our model. Comparison of the theoretical results with the experimental data shows that the large energy behaviour of the neutral fraction can be explained in terms of the pronounced downshift of the energy level caused by the short range interactions that are correctly contemplated in our model. The experimental trends observed for both Cu faces are also well reproduced by our model that accounts for the appropriate features of the density of states and work functions for both Cu(100) and Cu(111) surfaces.

The differences remaining between the theoretical and experimental results have to be mainly with surface energy gaps and long range interaction effects which are present in these Cu surfaces and that are not contemplated within our model calculation. The ion projectile state lying in the energy gap of the Cu(111) surface leads to an increase of the neutralization probability due to the blocking of electron loss processes. In the case of Cu(100) the presence of the image potential state ($n = 1$) originated by the long range interaction effects, can justify the dramatic increase of the neutralization probability at low energies due to the down shift of the projectile atom level caused by a bonding interaction.

Other charge state configurations of the Li atoms, such as excited and negative ion states can not be clearly disregarded in the interaction with the surface. These other neutralization channels are expected to be more probable in the case of the lowest work function surface, i.e. Cu(100).

Acknowledgements

The authors are very grateful to Vladimir Esaulov and Hicham Hamoudi for helpful discussions. This work was supported by ANPCyT through PICT14730 and 14724, CONICET through PIP5277, and U.N.L. through CAI+D grants.

References

[1] J. Loss, J.J.C. Geerlings, Phys. Rep. 190 (1990) 133.
[2] P. Nordlander, J.C. Tully, Phys. Rev. B42 (1990) 5564.
[3] E.R. Behringer, D.R. Anderson, B.H. Cooper, J.B. Marston, Phys. Rev. B54 (1996) 14765.
[4] C.A. Keller, C.A. DiRubio, G.A. Kimmel, B.H. Cooper, Phys. Rev. Lett. 75 (1995) 1654.
[5] G.A. Kimmel, B.H. Cooper, Phys. Rev. B48 (1993) 12164.
[6] A.G. Borisov, D. Teillet-Billy, J.P. Gauyacq, H. Winter, D. Dierkes, Phys. Rev. B54 (1996) 17166.
[7] D.G. Goryunov, A.G. Borisov, G.E. Makhmetov, D. Teillet-Billy, J.P. Gauyacq, Surf. Sci. 401 (1998) 206.
[8] M.J. Ashwim, D.P. Woodruff, Surf. Sci. 244 (1991) 247.
[9] J.B. Marston, D.R. Andersson, E.R. Behringer, B.H. Cooper, C.A. DiRubio, G.A. Kimmel, C. Richardson, Phys. Rev. B48 (1993) 7809.
[10] C.B. Weare, J.A. Yarmoff, Surf. Sci. 348 (1996) 359.
[11] K.A.H. German, C.B. Weare, P.R. Varekamp, J.A. Yarmoff, Phys. Rev. Lett. 70 (1993) 3510.
[12] K. Niedfeldt, E.A. Carter, P. Nordlander, J. Chem. Phys. 121 (2004) 3751.
[13] Keith Niedfeldt, Emily A. Carter, Peter Nordlander, Surf. Sci. 600 (2006) L291.
[14] Keith Niedfeldt, Peter Nordlander, Emily A. Carter, Phys. Rev. B74 (2006) 115109.
[15] A.R. Canario, T. Kravchuk, V.A. Esaulov, New J. Phys. 8 (2006) 227.
[16] T. Kravchuk, Yu. Bandourine, A. Hoffman, V.A. Esaulov, Surf. Sci. 600 (2006) L265.
[17] A.R. Canario, A.G. Borisov, J.P. Gauyacq, V.A. Esaulov, Phys. Rev. B71 (2005) 121401-1/4.
[18] A.G. Borisov, A.K. Kazansky, J.P. Gauyacq, Phys. Rev. Lett. 80 (1998) 1996.
[19] A.G. Borisov, A.K. Kazansky, J.P. Gauyacq, Phys. Rev. B59 (1999) 10935.
[20] A.G. Borisov, J.P. Gauyacq, E.V. Chulkov, V.M. Silkin, P.M. Echenique, Phys. Rev. B65 (2002) 235432.
[21] Hicham Hamoudi, Céline Dablemont, Vladimir A. Esaulov, Surf. Sci. 602 (2008) 2486.
[22] A.L. Boers, Nucl. Instr. Meth. Phys. Res. B2 (1984) 353.
[23] N.E. Bickers, Rev. Mod. Phys. 59 (1987) 845.
[24] P.M. Echenique, J.B. Pendry, Prog. Surf. Sci. 32 (1990) 111.
[25] E.V. Chulkov, V.M. Silkin, P.M. Echenique, Surf. Sci. 437 (1999) 330.
[26] F. Bonetto, M.A. Romero, Evelina A. García, R.A. Vidal, J. Ferrón, E.C. Goldberg, Phys. Rev. B78 (2008) 075422-1/7.
[27] P.G. Bolcatto, E.C. Goldberg, M.C.G. Passeggi, Phys. Rev. B 58 (1998) 5007.
[28] M.C. Torralba, P.G. Bolcatto, E.C. Goldberg, Phys. Rev. B 68 (2003) 075406.
[29] E.C. Goldberg, F. Flores, R.C. Monreal, Phys. Rev. B 71 (2005) 035112.
[30] M.A. Romero, E.C. Goldberg, Phys. Rev. B74 (2006) 195419.
[31] S. Huzinaga, J. Chem. Phys. 42 (1965) 1293;
S. Huzinaga, J. Andzelm, M. Klobukowsky, E. Radzio-Andzelm, Y. Sakai, H. Tatewaki, in: S. Huzinaga (Ed.), Gaussian Basis Set for Molecular Calculation, Elsevier, Ámsterdam, 1984.
[32] N.V. Smith, C.T. Chen, M. Weinert, Phys. Rev. B40 (1989) 7565.
[33] J.P. James, K.R. Glaeseman, G.A. Voth, J. Fritsch, A.A. Demkov, J. Ortega, O.F. Sankey, Phys. Rev. B 64 (2001) 195103;
P. Jelinek, H. Wang, J.P. Lewis, O.F. Sankey, J. Ortega, Phys. Rev. B 71 (2005) 235101.
[34] W. More, J. Merino, R. Monreal, P. Pou, F. Flores, Phys. Rev. B58 (1998) 7385.
[35] J.C. Lancaster, F.J. Kontur, G.K. Walters, F.B. Dunning, Phys. Rev. B67 (2003) 115413.
[36] S. Wethekam, H. Winter, Surf. Sci. 596 (2005) L319.
[37] F. Bonetto, M. Romero, Evelina A. García, R. Vidal, J. Ferrón, E.C. Goldberg, Europhys. Lett. 80 (2007) 53002.
[38] T. Hecht, H. Winter, A.G. Borisov, J.P. Gauyacq, A.K. Kazanky, Phys. Rev. Lett. 84 (2000) 2517.
[39] M. Maazouz, A.G. Borisov, V.A. Esaulov, J.P. Gauyacq, L. Guillemot, S. Lacombe, D. Teillet-Billy, Phys. Rev. B55 (1997) 13869.
[40] J. Zhao, N. Pontius, A. Winkelmann, V. Sametoglu, A. Kubo, A.G. Borisov, D. Sánchez-Portal, V.M. Silkin, E.V. Chulkov, P.M. Echenique, H. Petek, Phys. Rev. B78 (2008) 085419.
[41] H. Ishida, Phys. Rev. B38 (1988) 8006.
[42] N.B. Luna, F.J. Bonetto, R.A. Vidal, J. Ferrón, E.C. Goldberg, J. Mol. Catalysis A: Chemical 281 (2008) 237.